Anderson localization in Liouville space: The effective dephasing approximation

Roger F. Loring,* Daniel S. Franchi, and Shaul Mukamel
Department of Chemistry, University of Rochester, Rochester, New York 14627
(Received 18 May 1987)

The effective dephasing approximation (EDA) provides a self-consistent procedure for calculating the transport properties of a quantum particle in a disordered medium. It is based on mapping the averaged Liouville-space propagator into the propagator of a particle moving in an ordered lattice with an effective frequency-dependent dephasing rate. The effective dephasing rate is determined self-consistently. The Liouville equation for the averaged density matrix is isomorphic to a linearized Boltzmann equation, and the effective dephasing rate represents a generalized Bhatnagar-Gross-Krook strong-collision operator. The EDA is applied to the calculation of the ac conductivity of a particle governed by a tight-binding Hamiltonian with static diagonal disorder (the Anderson model). Our results agree with the predictions of scaling theories of the Anderson transition.

I. INTRODUCTION

The Anderson model is the most basic model for the motion of a quantum particle in a random potential that exhibits a transition from localized to delocalized states (a metal-nometal transition).[1-6] Anderson's original treatment, which is based on a resummation of the perturbation series of the wave function, dealt with the transition from a localized to a delocalized wave function as the degree of disorder is varied.[1] Other approaches that have been used to investigate Anderson localization include the coherent potential approximation[7,8] and renormalization-group and scaling techniques.[9-13] Most of these treatments focus on the calculation of the wave function or some of its properties, such as the participation ratio. Some recent works focused, on the other hand, on the direct calculation of transport properties.[14-17] We have recently developed a novel approach to localization problems, which focuses on the ensemble-averaged density matrix, rather than on wave function.[18,19] The effective dephasing approximation (EDA) yields a self-consistent mode-coupling equation in Liouville space that provides a simple and systematic method to calculate transport properties of a quantum particle in a disordered medium.[19] In the EDA, the Liouville equation for the ensemble-averaged density matrix is mapped onto the equation of motion of a particle whose dynamics are characterized by a frequency-dependent dephasing rate $\Gamma(\epsilon)$. $\Gamma(\epsilon)$ is determined self-consistently. The transport properties at long times are determined by the behavior of $\Gamma(\epsilon)$ for small ϵ. If $\Gamma=0$, the particle undergoes coherent motion on an ordered lattice. In this limit, the system is characterized by extended Bloch states. If Γ is large but finite, the motion is diffusive (incoherent) and can be described by a Pauli master equation. If $\Gamma(\epsilon)$ has an infrared divergence, $\Gamma(\epsilon)\sim\epsilon^{-1}$, the particle is localized. The signature of the metal-nonmetal transition is the transition from a dephasing rate that is finite at small frequencies to one that displays an infrared divergence.

In a previous work, we introduced the EDA and applied it to the motion of excitons in a disordered molecular crystal.[19] We calculated the observable in a transient grating experiment for a crystal characterized by the Anderson Hamiltonian, and demonstrated that four-wave-mixing spectroscopy provides a sensitive probe of the optical analog of a metal-nonmetal transition.[19] We have shown that the predictions of the EDA agree with the results of scaling theories of localization.[6,9] The EDA is an analytical method that provides a new perspective on the phenomenon of localization. Because it focuses on the density matrix rather than on the wave function, the EDA has the potential to treat classical as well as quantum systems. It has been recognized in recent years that classical systems, such as light propagating in a disordered medium, may exhibit a localization-delocalization transition that is analogous to the Anderson transition.[20-22] In this paper we review the critical behavior predicted by the EDA and present calculations of the electrical conductivity over a broad range of frequency scales and degrees of disorder.

II. THE EFFECTIVE LIOUVILLIAN: A GENERALIZED STRONG-COLLISION OPERATOR

We consider a quantum particle whose motion on a lattice is described by the tight-binding Hamiltonian

$$H=\sum_{\mathbf{x}} E_{\mathbf{x}}\,|\,\mathbf{x}\rangle\langle\,\mathbf{x}\,|+\sum_{\mathbf{x}\neq\mathbf{x}'}\hbar J(\mathbf{x}-\mathbf{x}')\,|\,\mathbf{x}\rangle\langle\,\mathbf{x}'\,|\ . \quad (2.1)$$

$|\,\mathbf{x}\rangle$ denotes the state in which the particle is localized at the lattice point $\mathbf{x}$. $J(\mathbf{x}-\mathbf{x}')$ is the transfer matrix element between sites and $E_{\mathbf{x}}$ is the particle energy at site $\mathbf{x}$. In the Anderson model of diagonal disorder, $\{E_{\mathbf{x}}\}$ are independent random variables with a distribution $P(E_{\mathbf{x}})$. The density matrix of the particle obeys the Liouville equation

$$\dot{\rho}=\frac{-i}{\hbar}[H,\rho]=-iL\rho\ . \quad (2.2)$$

It is convenient to change variables from $\mathbf{x}$ and $\mathbf{x}'$ to $\mathbf{r}$ and $\mathbf{s}$, which are defined by

$$\mathbf{x}=\mathbf{r}-\mathbf{s}/2 , \tag{2.3a}$$

$$\mathbf{x}'=\mathbf{r}+\mathbf{s}/2 . \tag{2.3b}$$

The density matrix element $\rho(\mathbf{r},\mathbf{s},t)$ is defined by

$$\rho(\mathbf{r},\mathbf{s},t)\equiv\langle \mathbf{r}-\mathbf{s}/2\,|\,\rho\,|\,\mathbf{r}+\mathbf{s}/2\rangle . \tag{2.4}$$

$\rho(\mathbf{r},0,t)$ is a diagonal element of the density matrix, and gives the probability that the particle is located at position $\mathbf{r}$ at time t. For $\mathbf{s}\neq 0$, $\rho(\mathbf{r},\mathbf{s},t)$ is a coherence that carries information on the phase relationship between two sites separated by a displacement $\mathbf{s}$. Substitution of Eq. (2.4) into Eq. (2.2) yields the equation of motion of $\rho(\mathbf{r},\mathbf{s},t)$:

$$\dot{\rho}(\mathbf{r},\mathbf{s},t)=-i\sum_{\mathbf{a}}J(\mathbf{a})[\rho(\mathbf{r}+\mathbf{a}/2,\mathbf{s}-\mathbf{a},t)-\rho(\mathbf{r}+\mathbf{a}/2,\mathbf{s}+\mathbf{a},t)] -i\hbar^{-1}(E_{\mathbf{r}-\mathbf{s}/2}-E_{\mathbf{r}+\mathbf{s}/2})\rho(\mathbf{r},\mathbf{s},t) . \tag{2.5}$$

The index $\mathbf{a}$ runs over all displacements in the lattice. The second term in Eq. (2.5) represents the effects of the random energies, and vanishes if the sites have identical energies.

Our goal is the calculation of the ensemble-averaged density matrix $\sigma(\mathbf{r},\mathbf{s},t)$:

$$\sigma(\mathbf{r},\mathbf{s},t)\equiv\langle\rho(\mathbf{r},\mathbf{s},t)\rangle . \tag{2.6}$$

The angular brackets in Eq. (2.6) represent an average over the random site energies. The effective dephasing approximation is based on the following ansatz for the form of the equation of motion of $\sigma(\mathbf{r},\mathbf{s},t)$:

$$\dot{\sigma}(\mathbf{r},\mathbf{s},t)=-i\sum_{\mathbf{a}}J(\mathbf{a})[\rho(\mathbf{r}+\mathbf{a}/2,\mathbf{s}-\mathbf{a},t)-\rho(\mathbf{r}+\mathbf{a}/2,\mathbf{s}+\mathbf{a},t)] -\int_0^t d\tau\hat{\Gamma}(t-\tau)[\sigma(\mathbf{r},\mathbf{s},\tau)-\hat{f}(\mathbf{s})\sigma(\mathbf{r},0,\tau)] . \tag{2.7}$$

The first term in Eq. (2.7) is identical to the first term in Eq. (2.5) and describes motion on a translationally invariant lattice. The second term accounts for the disorder and contains two functions which remain to be specified, $\hat{\Gamma}(t)$ and $\hat{f}(\mathbf{s})$. If we choose $\hat{\Gamma}(t)$ to decay rapidly on all relevant time scales, $\hat{\Gamma}(t)=\gamma\delta(t)$, and choose $\hat{f}(\mathbf{s})=\delta_{s,0}$, then Eq. (2.7) reduces to the Haken-Strobl equation of motion for the density matrix of an exciton in a disordered molecular crystal.[23] For this choice of $\hat{\Gamma}(t)$ and $\hat{f}(\mathbf{s})$, the second term in Eq. (2.7) causes all coherences $\rho(\mathbf{r},\mathbf{s},t)$ for $\mathbf{s}\neq 0$ to decay with a dephasing rate γ. Thus $\hat{\Gamma}(t)$ can be viewed as a generalized time-dependent dephasing rate. We can gain further insight into the physical significance of $\hat{\Gamma}(t)$ and $\hat{f}(s)$ by transforming to the Wigner representation.[24,25] The Wigner phase-space distribution function $\phi(\mathbf{r},\mathbf{p},t)$ is defined by

$$\phi(\mathbf{r},\mathbf{p},t)=N^{-1}\sum_{\mathbf{s}}\exp(i\mathbf{p}\cdot\mathbf{s}/\hbar)\sigma(\mathbf{r},\mathbf{s},t) . \tag{2.8}$$

N is the number of lattice sites. Equation (2.8) is the discretized version of the usual Wigner function, in which $\mathbf{r}$ and $\mathbf{p}$ are continuous variables.[24,25] Applying the Wigner transform in Eq. (2.8) to Eq. (2.7) yields the equation of motion of $\phi(\mathbf{r},\mathbf{p},t)$:

$$\dot{\phi}(\mathbf{r},\mathbf{p},t)=2\sum_{\mathbf{a}}J(\mathbf{a})\sin(\mathbf{p}\cdot\mathbf{a}/\hbar)\phi(\mathbf{r}+\mathbf{a}/2,\mathbf{p},t) +\int_0^t d\tau\hat{\Gamma}(t-\tau)\sum_{\mathbf{p}'}[f(\mathbf{p})\phi(\mathbf{r},\mathbf{p}',\tau)-f(\mathbf{p}')\phi(\mathbf{r},\mathbf{p},\tau)] , \tag{2.9a}$$

$$f(\mathbf{p})=N^{-1}\sum_{\mathbf{s}}\exp(i\mathbf{p}\cdot\mathbf{s}/\hbar)\hat{f}(\mathbf{s}) . \tag{2.9b}$$

$f(\mathbf{p})$, the Wigner transform of $\hat{f}(\mathbf{s})$, is normalized according to

$$\hat{f}(0)=\sum_{\mathbf{p}}f(\mathbf{p})=1 . \tag{2.10}$$

The first term in Eq. (2.9a) represents the free motion of the particle on an ordered lattice. If we take $\hat{\Gamma}(t)=\gamma\delta(t)$, then the second term has the form of the Bhatnagar-Gross-Krook (BGK) strong-collision operator in the Boltzmann equation, in which γ is the collision rate and $f(\mathbf{p})$ is the distribution of momenta after a collision.[26,27] The transformation to the Wigner representation shows that the generalized dephasing rate $\hat{\Gamma}(t)$ can be regarded as a generalized collision rate in the Boltzmann equation. Equation (2.9a) has the form of a discretized Boltzmann equation. If the transfer matrix element $J(\mathbf{r})$ is taken to have the value J for nearest-neighbor sites and to vanish otherwise, then in the continuum limit, $\mathbf{p}\cdot\mathbf{a}/\hbar\rightarrow 0$, Eq. (2.9a) becomes

$$\dot{\phi}(\mathbf{r},\mathbf{p},t)=(\mathbf{p}/m)\cdot[\nabla\phi(\mathbf{r},\mathbf{p},t)] +\int_0^t d\tau\hat{\Gamma}(t-\tau)\int d\mathbf{p}'[F(\mathbf{p})\phi(\mathbf{r},\mathbf{p}',\tau)-F(\mathbf{p}')\phi(\mathbf{r},\mathbf{p},\tau)] , \tag{2.11a}$$

$$m=\hbar/(2Jl^2) . \tag{2.11b}$$

In Eq. (2.11b), l is the lattice spacing. $F(\mathbf{p})$ is defined in analogy to $f(\mathbf{p})$, but has continuum normalization:

$$\int F(\mathbf{p})d\mathbf{p}=1 . \tag{2.11c}$$

Equation (2.11a) has the form of the Boltzmann equation in the BGK approximation of a classical particle of mass m with a generalized collision rate $\hat{\Gamma}(t)$.[26,27]

We next turn to the calculation of the density matrix σ, which can be determined either by solving Eq. (2.7), or by solving Eq. (2.9a) and inverting the Wigner transform. We shall work directly with Eq. (2.7). The Fourier-Laplace transform of $\sigma(\mathbf{r},\mathbf{s},t)$ is defined to be

$$\hat{\sigma}(\mathbf{k},\mathbf{s},\epsilon)=N^{-1/2}\sum_{\mathbf{r}}\int_0^\infty dt\exp(-\epsilon t+i\mathbf{k}\cdot\mathbf{r})\sigma(\mathbf{r},\mathbf{s},t) , \tag{2.12}$$

and the Liouville-space Green's function G is given by

$$\hat{\sigma}(\mathbf{k},\mathbf{s},\epsilon)=\sum_{\mathbf{s}'} G_{\mathbf{s}\mathbf{s}'}(\mathbf{k},\epsilon)\sigma(\mathbf{k},\mathbf{s}',0) . \tag{2.13}$$

We have developed a novel procedure based on the Liouville-space t matrix, by which $G_{\mathbf{s}\mathbf{s}'}(\mathbf{k},\epsilon)$ can be obtained in closed form.[19] This method is described in Appendix A of Ref. 19. The final result is

$$G_{\mathbf{s}\mathbf{s}'}(\mathbf{k},\epsilon)=G^{(0)}_{\mathbf{s}\mathbf{s}'}(\mathbf{k},\epsilon)+G^{(0)}_{\mathbf{0}\mathbf{s}'}(\mathbf{k},\epsilon)K_{\mathbf{s}}(\mathbf{k},\epsilon) \times\Gamma(\epsilon)/[1-\Gamma(\epsilon)K_{\mathbf{0}}(\mathbf{k},\epsilon)] , \tag{2.14a}$$

where

$$K_{\mathbf{s}}(\mathbf{k},\epsilon)=\sum_{\mathbf{s}'}\hat{f}(\mathbf{s}')G^{(0)}_{\mathbf{s}\mathbf{s}'}(\mathbf{k},\epsilon) , \tag{2.14b}$$

and

$$G^{(0)}_{\mathbf{s}\mathbf{s}'}(\mathbf{k},\epsilon)=N^{-1}\sum_{\mathbf{q}}\exp[i\mathbf{q}\cdot(\mathbf{s}-\mathbf{s}')]\left[\epsilon+\Gamma(\epsilon)+2\sum_{\mathbf{a}}\exp(i\mathbf{q}\cdot\mathbf{a})J(\mathbf{a})\sin(\mathbf{k}\cdot\mathbf{a}/2)\right]^{-1} . \tag{2.14c}$$

The frequency-dependent collision rate $\Gamma(\epsilon)$ is the Laplace transform of $\hat{\Gamma}(t)$:

$$\Gamma(\epsilon)=\int_0^\infty dt\,\exp(-\epsilon t)\hat{\Gamma}(t) . \tag{2.15}$$

In the present work, we shall make the following choice for $f(\mathbf{p})$, the equilibrium momentum distribution:

$$f(\mathbf{p})=\begin{cases}1/N & \text{if } \mathbf{p} \text{ is in the first Brillouin zone} ,\\ 0 & \text{otherwise} .\end{cases} \tag{2.16}$$

Inverting the Wigner transform in Eq. (2.9b) shows that this choice of $f(\mathbf{p})$ implies that

$$\hat{f}(\mathbf{s})=\delta_{\mathbf{s},\mathbf{0}} . \tag{2.17}$$

According to Eq. (2.16), the momentum is uniformly distributed after each collision. For this choice of $\hat{f}(\mathbf{s})$, the general expression in Eq. (2.14) reduces to

$$G_{\mathbf{s}\mathbf{s}'}(\mathbf{k},\epsilon)=G^{(0)}_{\mathbf{s}\mathbf{s}'}(\mathbf{k},\epsilon)+G^{(0)}_{\mathbf{s}\mathbf{0}}(\mathbf{k},\epsilon)G^{(0)}_{\mathbf{0}\mathbf{s}'}(\mathbf{k},\epsilon) \times\Gamma(\epsilon)/[1-\Gamma(\epsilon)Q(\mathbf{k},\epsilon)] , \tag{2.18a}$$

with

$$Q(\mathbf{k},\epsilon)=G^{(0)}_{\mathbf{0}\mathbf{0}}(\mathbf{k},\epsilon) . \tag{2.18b}$$

The transport properties of the quantum particle can be determined from $P(\mathbf{r},t)$, the probability that the particle undergoes a displacement $\mathbf{r}$ in time t. $\hat{P}(\mathbf{k},\epsilon)$, the Fourier-Laplace transform [Eq. (2.12)] of $P(\mathbf{r},t)$ is related to the Green's function by

$$\hat{P}(\mathbf{k},\epsilon)=G_{\mathbf{0}\mathbf{0}}(\mathbf{k},\epsilon) . \tag{2.19}$$

The generalized wave vector and frequency-dependent diffusion coefficient $D(\mathbf{k},\epsilon)$ is defined by

$$\hat{P}(\mathbf{k},\epsilon)=[\epsilon+k^2D(\mathbf{k},\epsilon)]^{-1} , \tag{2.20}$$

and is related to $\Gamma(\epsilon)$ by

$$k^2D(\mathbf{k},\epsilon)=Q^{-1}(\mathbf{k},\epsilon)-\Gamma(\epsilon)-\epsilon . \tag{2.21}$$

If $D(\mathbf{k},\epsilon)$ approaches a finite value $D(0,0)$ for small ϵ and $\mathbf{k}$, then in this limit $\hat{P}(\mathbf{k},\epsilon)$ assumes the form of the propagator of a diffusion equation with diffusion constant $D(0,0)$. Equation (2.21) shows that if $\Gamma(\epsilon)$ approaches a finite limit for small frequencies, then $D(0,0)$ exists, and transport is diffusive at long times and for large displacements. Let us consider the implications of an infrared divergence of $\Gamma(\epsilon)$: $\Gamma(\epsilon)\sim\epsilon^{-\alpha}$. For $\Gamma(\epsilon)\gg J(\mathbf{a})$, Eq. (2.21) becomes

$$k^2D(\mathbf{k},\epsilon)=\{4/[\epsilon+\Gamma(\epsilon)]\}\sum_{\mathbf{a}}J^2(\mathbf{a})\sin^2(\mathbf{k}\cdot\mathbf{a}/2) . \tag{2.22}$$

For an isotropic lattice in which the small wave-vector limit of $D(\mathbf{k},\epsilon)$ is independent of the direction of $\mathbf{k}$, the $\mathbf{k}\to\mathbf{0}$ limit of Eq. (2.22) in d dimensions is

$$D(0,\epsilon)=\{d[\epsilon+\Gamma(\epsilon)]\}^{-1}\sum_{\mathbf{a}}a^2J^2(\mathbf{a}) . \tag{2.23}$$

Equation (2.23) shows that if $\Gamma(\epsilon)$ has an infrared divergence, $\Gamma(\epsilon)\sim\epsilon^{-\alpha}$, then $D(0,\epsilon)$ vanishes as ϵ^α. The mean-squared displacement of the particle $\langle r^2(t)\rangle$ is related to the diffusion coefficient by

$$\int_0^\infty dt\,\exp(-\epsilon t)\langle r^2(t)\rangle=2d\epsilon^{-2}D(0,\epsilon) . \tag{2.24}$$

Application of the Tauberian theorem for Laplace transforms shows that if $D(0,\epsilon)$ vanishes as ϵ^α, then $\langle r^2(t)\rangle$ is proportional to $t^{1-\alpha}$. If $\alpha=1$, then $\langle r^2(t)\rangle$ reaches a finite limit at long times, and the particle is localized. For $0<\alpha<1$, $\langle r^2(t)\rangle$ is unbounded but increases more slowly than in the diffusive case ($\alpha=0$). The case in which $0<\alpha<1$ is known as weak localization.[28]

The complex electrical conductivity $\sigma(\omega)$ is related to the diffusion coefficient by [18(b)]

$$\sigma(\omega)=(ne^2/kT)D(0,i\omega) , \tag{2.25a}$$

$$\sigma(\omega)=\sigma'(\omega)+i\sigma''(\omega) . \tag{2.25b}$$

$\sigma'(\omega)$ and $\sigma''(\omega)$ are the real and imaginary parts of the complex conductivity, respectively, n is the number density of charge carriers, and e is the magnitude of their electrical charge. The ac conductivity is proportional to $\sigma'(\omega)$. If $\alpha=1$, then $\sigma'(\omega)\sim\omega$ for small frequencies, and the system has zero dc conductivity. If $\alpha=0$, the dc conductivity is finite. Thus, the existence of a metal-insulator phase transition implies critical behavior for $\Gamma(\epsilon)$. In the following section, we shall derive a self-

consistent equation for $\Gamma(\epsilon)$, which predicts such critical behavior and hence predicts the metal-insulator transition.

III. TRANSPORT PROPERTIES IN THE ANDERSON MODEL

The EDA self-consistent equation is obtained by focusing on two dynamical quantities: the frequency-dependent dephasing rate $\Gamma(\epsilon)$, and $P_0(\epsilon)$, the Laplace transform of $P(\mathbf{0},t)$. $P(\mathbf{0},t)$ is the ensemble-averaged probability that the particle is located at the same position at time t that it occupied at time 0. Inversion of the Fourier transform in Eq. (2.20) at $\mathbf{r}=0$ yields

$$P_0(\epsilon)=\Omega^{-1}\int d\mathbf{k}[\epsilon+k^2D(\mathbf{k},\epsilon)]^{-1} . \tag{3.1}$$

The integration in Eq. (3.1) is carried out over the first Brillouin zone, whose "volume" is Ω. $D(\mathbf{k},\epsilon)$ is related to $\Gamma(\epsilon)$ in Eq. (2.21). Substitution of Eq. (2.21) into Eq. (3.1) results in a relation between $\Gamma(\epsilon)$ and $P_0(\epsilon)$. In order to close the equation, we require a second relation between these two quantities. In Ref. 19, we derive an approximate relation between $\Gamma(\epsilon)$ and $P_0(\epsilon)$, which is based on their high-frequency expansions:

$$\Gamma(\epsilon)=\Gamma_0+2\Delta^2P_0(\epsilon) , \tag{3.2a}$$

$$\hbar^2\Delta^2=\int_{-\infty}^{\infty} dE\, E^2P(E) . \tag{3.2b}$$

$P(E)$ is the distribution of site energies, and $\hbar^2\Delta^2$ is its second moment. Equation (3.2a) includes a dephasing rate Γ_0 that is independent of frequency. Γ_0 accounts for dephasing that arises from processes that are not included in the Hamiltonian of Eq. (2.1), such as electron-phonon interactions. The results of the preceding section were derived for a transfer matrix element $J(\mathbf{a})$, with an unspecified dependence on the displacement $\mathbf{a}$. We now specialize to $J(\mathbf{a})$ that has the value J for nearest-neighbor sites and that vanishes otherwise. Combination of Eqs. (3.1) and (3.2) yields a closed equation for $\Gamma(\epsilon)$, the EDA self-consistent equation:

$$\Gamma(\epsilon)=\Gamma_0+2\Delta^2\Omega^{-1}\int d\mathbf{k}[Q(\mathbf{k},\epsilon)^{-1}-\Gamma(\epsilon)]^{-1} , \tag{3.3a}$$

$$Q(\mathbf{k},\epsilon)=\pi^{-d}\int_0^{\pi} dq_1\cdots\int_0^{\pi} dq_d\left[\epsilon+\Gamma(\epsilon)+4iJ\sum_{j=1}^{d}\sin(q_j)\sin(k_j/2)\right]^{-1} , \tag{3.3b}$$

$$k_j=\mathbf{k}\cdot\mathbf{x}_j . \tag{3.3c}$$

In Eq. (3.3c), $\mathbf{x}_j$ is the lattice vector in the jth direction. $Q(\mathbf{k},\epsilon)$ is defined for any $J(\mathbf{a})$ in Eq. (2.18b).

The EDA self-consistent equation predicts the existence of a critical point for $\Gamma(\epsilon)$ and the conductivity, and assumes a simple form in the vicinity of the critical point. If the particle is localized, the frequency-dependent diffusion coefficient $D(0,\epsilon)$ vanishes as ϵ approaches zero, which implies an infrared divergence in $\Gamma(\epsilon)$ [Eq. (2.23)]. If the particle is delocalized, $D(0,0)$ is finite, but becomes arbitrarily small in the vicinity of the critical point, which implies that $\Gamma(0)$ becomes arbitrarily large. Thus, in the vicinity of the transition, on either side of the critical point, the condition $\Gamma(\epsilon)\gg J$ is satisfied for sufficiently small ϵ. The form of the EDA equation in this limit can be derived by substituting Eq. (2.22) rather than Eq. (2.21) into Eq. (3.1). The result is

$$\Gamma(\epsilon)=\Gamma_0+\chi\{[\epsilon+\Gamma(\epsilon)]/2\}I_d\{\epsilon[\epsilon+\Gamma(\epsilon)]/4J^2\} , \tag{3.4a}$$

where

$$\chi=\Delta^2/J^2 . \tag{3.4b}$$

$I_d(y)$, the diagonal element of the Green's function of the d-dimensional analog of a simple-cubic lattice, is given by

$$I_d(y)=\pi^{-d}\int_0^{\pi} dk_1\cdots\int_0^{\pi} dk_d\left[y+d-\sum_{j=1}^{d}\cos(k_j)\right]^{-1} . \tag{3.5}$$

The argument of I_d in Eq. (3.4a) becomes arbitrarily small in the vicinity of the critical point, so that the behavior of the solution of Eq. (3.4a) near the transition can be determined from the limiting behavior of $I_d(y)$ for small y:[29–31]

$$\lim_{y\to 0} I_d(y)=\begin{cases}(2y)^{-1/2}, & d=1\\ -(2\pi)^{-1}\ln(y), & d=2\\ I_3(0)-\pi^{-1}(y/2)^{1/2}, & d=3\end{cases} \tag{3.6a}$$

$$I_3(0)\cong 0.5055 , \tag{3.6b}$$

Substitution of Eqs. (3.6a) into Eq. (3.4a), and solution of the resulting equation in one and two dimensions yields the following behavior for $\Gamma(\epsilon)$. At $\chi=0$, $\Gamma(\epsilon)=\Gamma_0$. For $\chi>0$, $\Gamma(\epsilon)$ diverges as ϵ^{-1} for small frequency. The implications of these results for the motion of the particle can be obtained from Eqs. (2.23) and (2.24). The particle is predicted to be localized in one and two dimensions for any finite disorder, in agreement with the scal-

ing theory of localization.[6] Our criterion for localization is the limiting behavior at long times of $\langle r^2(t)\rangle$, the mean-squared displacement. If $\langle r^2(t)\rangle$ is bounded for all times, the particle is considered to be localized, and if $\langle r^2(t)\rangle$ increases linearly in time, the particle is considered to be delocalized. If $\langle r^2(t)\rangle$ increases less strongly than linearly in time, the particle is weakly localized.[28] If the particle is localized, the dc conductivity is zero, and if the particle is delocalized, the dc conductivity is finite [Eq. (2.25a)]. Substitution of Eq. (3.6a) with $d=3$ into Eq. (3.4a) yields a self-consistent equation for $\Gamma(\epsilon)$, which is cubic in $\Gamma^{1/2}$, that is valid in the vicinity of the critical point in three dimensions:

$$[\Gamma(\epsilon)/\Gamma_0]\{1-\chi/\chi^*+(\chi/2\pi)[\epsilon\Gamma(\epsilon)/8J^2]^{1/2}\}=1. \quad (3.7)$$

Equation (3.4a) predicts a metal-insulator transition at $\chi=\chi^*$, where χ^* is given by

$$\chi^*=2/I_3(0)\cong 3.957 . \quad (3.8)$$

For $\chi>\chi^*$, $\Gamma(\epsilon)$ diverges as ϵ^{-1} as $\epsilon\to 0$. For $\chi<\chi^*$, $\Gamma(\epsilon)$ approaches a finite limit as $\epsilon\to 0$. At $\chi=\chi^*$, $\Gamma(\epsilon)$ diverges as $\epsilon^{-1/3}$. χ^* has been estimated by a variety of numerical methods for the original Anderson model, in which the site energies are uniformly distributed between $-W/2$ and $W/2$. Recent results for the critical value of W/J are 14.9 ± 0.4,[12] 14.5,[4] 19.0 ± 0.5,[11] 16.5 ± 0.5,[10] and 15.95 ± 0.25.[13] Our value of $\chi^*\cong 3.957$ corresponds to $(W/J)^*\cong 6.9$. The analytical EDA approach yields a prediction for χ^* that is within a factor of 2 of the current numerical predictions. Solving Eq. (3.7) for $\Gamma(\epsilon)$ allows us to calculate $D(0,\epsilon)$ from Eq. (2.23), $\langle r^2(t)\rangle$ from Eq. (2.24), and $P(0,t)$ from the inverse Laplace transform of Eq. (3.2a):

$$D(0,\epsilon)=\begin{cases}(2J^2l^2/\Gamma_0)(1-\chi/\chi^*), & \chi<\chi^*\\ l^2[(4\pi/\chi)(\chi/\chi^*-1)]^{-2}\epsilon, & \chi>\chi^*\\ l^2\{J^2\chi^*/[2^{3/2}\pi\Gamma_0]\}^{2/3}\epsilon^{1/3}, & \chi=\chi^*\end{cases} \quad (3.9)$$

$$P(0,t)\sim\begin{cases}t^{-3/2}(2\Delta^2)^{-1}(\chi/2\pi)\Gamma_0^{3/2}(8J^2)^{-1/2}(1-\chi/\chi^*)^{-5/2}, & \chi<\chi^*\\ 4(J/\Delta)^2[(2\pi/\chi)(\chi/\chi^*-1)]^2, & \chi>\chi^*\\ t^{-2/3}(2\Delta^2)^{-1}[2^{5/2}\pi\Gamma_0 J/\chi^*]^{2/3}, & \chi=\chi^*\end{cases} \quad (3.10)$$

$$\langle r^2(t)\rangle\sim\begin{cases}t[2J^2l^2(1-\chi/\chi^*)/\Gamma_0], & \chi<\chi^*\\ l^2[(4\pi/\chi)(\chi/\chi^*-1)]^{-2}, & \chi>\chi^*\\ t^{2/3}l^2\{J^2\chi^*/(2^{3/2}\pi\Gamma_0)\}^{2/3}, & \chi=\chi^* .\end{cases} \quad (3.11)$$

In the delocalized regime ($\chi<\chi^*$), the transport is diffusive at long times: $\langle r^2(t)\rangle$ increases linearly with time, and $P(0,t)$ decays as $t^{-3/2}$. In the localized regime ($\chi>\chi^*$), $\langle r^2(t)\rangle$ is bounded, and $P(0,t)$ decays to a nonzero value, indicating that there is a finite probability at all times that the particle is to be found at its original site. At the critical point ($\chi=\chi^*$), the particle is weakly localized. $\langle r^2(t)\rangle$ increases as $t^{2/3}$, and $P(0,t)$ decays as $t^{-2/3}$. For $\chi>\chi^*$, $D(0,\epsilon)$ is linear in ϵ for small ϵ, with a coefficient that diverges as $(\chi-\chi^*)^{-2\nu}$. For $\chi<\chi^*$, $D(0,\epsilon)$ approaches a constant value at small ϵ that vanishes as $(\chi^*-\chi)^s$. The critical exponents in Eq. (3.9) are $\nu=1$ and $s=1$, which obey the scaling relation of Wegner, $s=(d-2)\nu$.[9(a)] Numerical estimates of the exponent ν range from 0.6 to 1.8.[9(b),10–13] As discussed in Refs. 18 and 19, the critical exponents in Eqs. (3.9)–(3.11) are identical to those obtained by Vollhardt and Wolfle for a gas of noninteracting fermions at zero temperature in a random potential.[16] A comparison between their self-consistent equation for the diffusion kernel, which was derived with a diagrammatic approach, and Eq. (3.4a) is made in Ref. 18(a). The limiting behavior of the complex conductivity at small frequencies near the transition can be determined from Eqs. (2.25):

$$\begin{aligned}&\sigma'(\omega)=\sigma_0(1-\chi/\chi^*)+A_1(1-\chi/\chi^*)^{-1/2}\omega^{1/2}, && \chi<\chi^*\\ &\sigma''(\omega)=A_1(1-\chi/\chi^*)^{-1/2}\omega^{1/2}, && \chi<\chi^*\\ &\sigma'(\omega)=A_2(\chi/\chi^*-1)^{-5}\omega^2, && \chi>\chi^*\\ &\sigma''(\omega)=A_3(\chi/\chi^*-1)^{-2}\omega, && \chi>\chi^*\\ &\sigma'(\omega)=A_4\omega^{1/3}, && \chi=\chi^*\\ &\sigma''(\omega)=3^{1/2}\sigma'(\omega), && \chi=\chi^*\end{aligned} \quad (3.12a)$$

$$\begin{aligned}&\sigma_0=(ne^2/kT)(2J^2l^2/\Gamma_0) ,\\ &A_1=\sigma_0\chi\Gamma_0^{1/2}/(8\pi J) ,\\ &A_2=\sigma_0\chi^4\Gamma_0^2/(2^9\pi^4J^4) ,\\ &A_3=\sigma_0\chi^2\Gamma_0/(32\pi^2J^2) ,\\ &A_4=\sigma_0\Gamma_0^{1/3}/(16\pi J/\chi^*)^{2/3} .\end{aligned} \quad (3.12b)$$

The ac conductivity is proportional to $\sigma'(\omega)$. The dc conductivity is zero for $\chi\geq\chi^*$, and is finite for $\chi<\chi^*$.

The critical behavior of transport properties within the EDA can thus be determined analytically. We next turn to the calculation of transport properties for any

time scale and degree of disorder, using Eqs. (3.3). It is shown in Appendix D of Ref. 19 that $Q(\mathbf{k},\epsilon)$, which is written as a d-dimensional integral in Eq. (3.3b), can be expressed as the following one-dimensional integral over a product of d zeroth-order Bessel functions:

$$Q(\mathbf{k},\epsilon)=\int_0^\infty dy\,\exp\{-[\epsilon+\Gamma(\epsilon)]y\}\times\prod_{n=1}^{d}J_0[4J\sin(k_n/2)y]\ . \tag{3.13}$$

In order to solve Eq. (3.3a) for $\Gamma(\epsilon)$, one must carry out the integration in Eq. (3.13), substitute the result into Eq. (3.3a), and then carry out the d-dimensional integral in Eq. (3.3a). We shall make the following simplifying approximation in our numerical calculations. We shall choose $\mathbf{k}$ in a particular direction (e.g., $\mathbf{k}=k\hat{\mathbf{z}}$) in evaluating Eq. (3.13), resulting in

$$\begin{aligned}Q(k,\epsilon)&=\int_0^\infty dy\,\exp\{-[\epsilon+\Gamma(\epsilon)]y\}\times J_0[4J\sin(kl/2)y]\\&=\{[\epsilon+\Gamma(\epsilon)]^2+16J^2\sin^2(kl/2)\}^{-1/2}\ .\end{aligned} \tag{3.14}$$

We then replace $\int d\mathbf{k}$ in Eq. (3.3a) with $\int k^{d-1}dk$ to obtain an approximation to the EDA equation in which the number of integrations has been reduced from $2d$ to one:

$$\Gamma(\epsilon)=\Gamma_0+2d\Delta^2(l/\pi)^d\times\int_0^{\pi/l}k^{d-1}dk\{[Q(k,\epsilon)]^{-1}-\Gamma(\epsilon)\}^{-1}\ . \tag{3.15}$$

It is easily verified that the critical exponents predicted by Eq. (3.15) are identical to those obtained from Eq. (3.3). In the limit $\Gamma(\epsilon)\gg J$, Eq. (3.15) reduces to a form identical to that of Eq. (3.4), with the diagonal Green's function $I_d(y)$ in Eq. (3.5) replaced by $\tilde{I}_d(y)$:

$$\tilde{I}_d(y)=d\pi^{-d}\int_0^\pi q^{d-1}dq[y+(1-\cos q)]^{-1}\ . \tag{3.16}$$

For $d=1$, $\tilde{I}_d(y)=I_d(y)$, and for $d>1$, $\tilde{I}_d(y)$ is an approximation to $I_d(y)$. The limiting behavior of $\tilde{I}_d(y)$ for small y is

$$\lim_{y\to 0}\tilde{I}_d(y)=\begin{cases}(2y)^{-1/2}, & d=1\\ -(2/\pi^2)\ln(y), & d=2\\ \tilde{I}_3(0)-(3/\pi^2)(2y)^{1/2}, & d=3\end{cases} \tag{3.17a}$$

$$\tilde{I}_3(0)=(12/\pi^2)\ln 2\cong 0.8428\ . \tag{3.17b}$$

The functional dependence of $\tilde{I}_d(y)$ on y for small y is identical to that of $I_d(y)$ in Eq. (3.6), although the numerical prefactors are different for $d>1$. Therefore, the critical exponents predicted by Eq. (3.15) are identical to those determined from Eq. (3.3), although the numerical values of the critical point in $d=3$ are different. Equation (3.15) predicts a critical point in $d=3$ at $\chi^*=2/\tilde{I}_3(0)\cong 2.373$, which should be compared with $\chi^*=3.957$ in Eq. (3.8). Equation (3.15) represents a reasonable approximation to Eq. (3.3a) that can be used to investigate qualitatively the behavior of transport properties within the Anderson model. Calculations of transport properties from the solution of Eq. (3.15) for $d=3$ are depicted in Figs. 1–7.

Figure 1 illustrates the behavior of $P(0,t)$ in $d=3$ for $\chi=1.00$, 1.75, 2.50, 3.25, and 4.00. The intrinsic dephasing Γ_0 is taken to equal $2J$ in all of the figures. For $\chi>\chi^*\cong 2.373$, $P(0,t)$ decays to a nonzero limiting value, indicating that the particle is localized. For $\chi<\chi^*$, $P(0,t)$ decays to zero, which is a signature of a delocalized particle. At a given value of t, $P(0,t)$ increases with increasing χ. $P(0,t)$ is shown in Fig. 2 for a set of χ in the vicinity of χ^*: $\chi=2.00$, 2.25, χ^*, 2.75, and 3.00. The calculations of Figs. 1 and 2 were carried out by using Eq. (3.2a) to convert Eq. (3.15) to a closed equation for $P_0(\epsilon)$. This equation was solved numerically, and the Laplace transform was inverted using the Stehfest algorithm.[32] Calculations of the real and imaginary parts of the complex conductivity $\sigma(\omega)$ are shown in Figs. 3–7. These calculations were carried out as follows. $\sigma(\omega)$ is related to $D(0,i\omega)$ in Eq. (2.25a). From Eqs. (2.23) and (3.2a), $D(0,i\omega)$ is related to $P_0(i\omega)$ by

$$D(0,i\omega)=2J^2l^2/[i\omega+\Gamma_0+2\Delta^2P_0(i\omega)]\ . \tag{3.18}$$

$P_0(\epsilon)$ was determined self-consistently from Eq. (3.15), and the Laplace transform was inverted numerically to obtain $P(0,t)$. $P_0(i\omega)$ was determined from $P(0,t)$ by performing a fast Fourier transform, which was carried

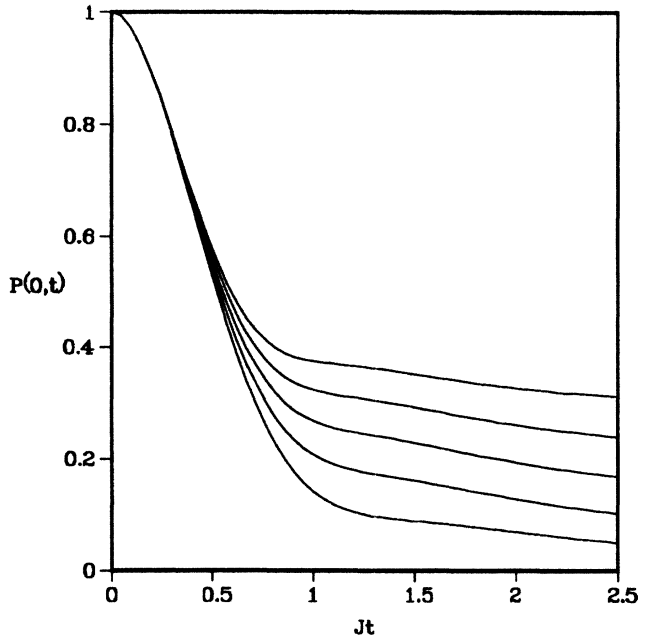

FIG. 1. $P(0,t)$, the probability that an electron occupies its initial site at time t, is calculated from Eq. (3.15) for the Anderson model in three dimensions. The disorder variable χ for the various curves (from bottom to top) takes the values 1.00, 1.75, 2.50, 3.25, and 4.00. The transition occurs at $\chi^*\cong 2.373$. On the insulating side ($\chi>\chi^*$), $P(0,t)$ decays to a finite value at long times, indicating that the electron is localized. On the conducting side ($\chi<\chi^*$), $P(0,t)$ decays as $t^{-3/2}$ at long times. $\Gamma_0/J=2$.

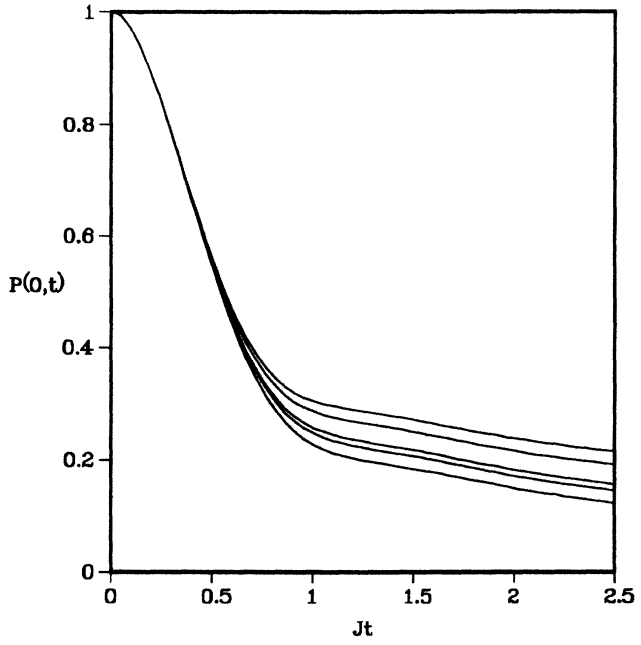

FIG. 2. $P(0,t)$, the probability that an electron occupies its initial site at time t, is calculated from Eq. (3.15) in three dimensions. The disorder variable χ for the various curves (from bottom to top) takes the values 2.00, 2.25, 2.373, 2.75, and 3.00. The transition occurs at $\chi^* \cong 2.373$. On the insulating side ($\chi > \chi^*$), $P(0,t)$ decays to a finite value at long times, indicating that the electron is localized. On the conducting side ($\chi < \chi^*$), $P(0,t)$ decays as $t^{-3/2}$ at long times. At $\chi = \chi^*$, $P(0,t)$ decays as $t^{-2/3}$. $\Gamma_0/J = 2$.

out with a time step of $J\Delta t = 0.048$, which yields a frequency step of $\Delta\omega/J = 0.001$. $\sigma'(\omega)$ and $\sigma''(\omega)$ were calculated by substituting this result into Eqs. (3.18) and (2.25). In Figs. 3–6, $\sigma'(\omega)$ and $\sigma''(\omega)$ in $d = 3$ are expressed in units of $\sigma_0 = (ne^2/kT)(2J^2l^2/\Gamma_0)$. The behavior of $\sigma'(\omega)$, which is proportional to the ac conductivity, is shown in Fig. 3(a) (linear plot) and Fig. 3(b) (logarithmic plot) for a range of χ both above and below $\chi^* \cong 2.373$. Each curve is marked with the appropriate value of χ. The power-law frequency dependence of $\sigma'(\omega)$ in different frequency regimes is clearly illustrated in the logarithmic plots in Fig. 3(b). For $\omega/J \gg 1$, the ac conductivity decays as ω^{-2} for $\chi > \chi^*$, $\chi < \chi^*$, and $\chi = \chi^*$. The asymptotic behavior for $\omega/J \ll 1$ is given in Eq. (3.12a). On the metallic side of the transition ($\chi < \chi^*$), the ac conductivity approaches a nonzero value at small frequencies, and has the form $\sigma'(\omega) = \alpha + \beta\omega^{1/2}$. On the insulating side of the transition ($\chi > \chi^*$), the ac conductivity approaches zero as ω^2. Calculations of the imaginary part of the complex conductivity $\sigma''(\omega)$ are shown in Fig. 4 for the same values of χ that were used in Fig. 3. The transition in $\sigma''(\omega)$, as χ is varied across the critical point, is less dramatic than the corresponding transition in $\sigma'(\omega)$, since $\sigma''(\omega)$ approaches zero for small frequencies on both sides of the transition, as can be seen from Eq. (3.12a). For $\chi > \chi^*$, $\sigma''(\omega)$ vanishes as ω; for $\chi < \chi^*$, $\sigma''(\omega)$ vanishes as $\omega^{1/2}$; and at $\chi = \chi^*$, it vanishes as $\omega^{1/3}$. In Figs. 5(a) and 5(b), the ac conductivity is shown for a range of χ in the vicinity of χ^* on linear and logarithmic plots. At $\chi = \chi^*$, the ac conductivity is proportional to $\omega^{1/3}$ for $\omega/J \ll 1$. In Fig. 6, $\sigma''(\omega)$ is shown for the same values of χ that were used in Fig. 5(a). The dc conductivity $\sigma'(0)$ is shown as a

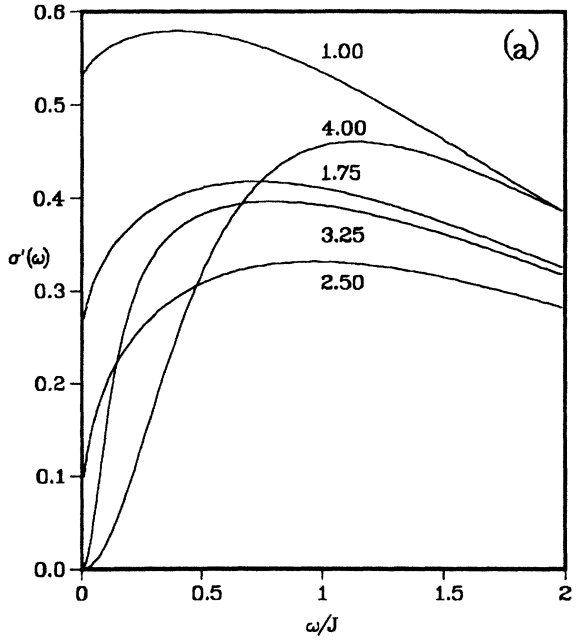

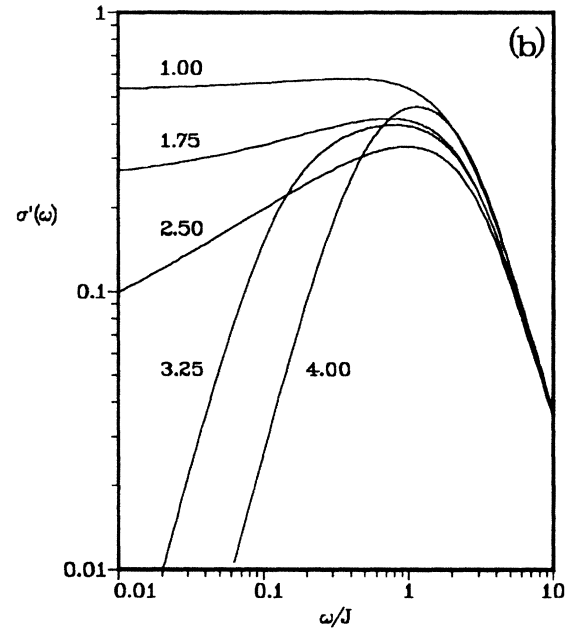

FIG. 3. (a) The ac conductivity $\sigma'(\omega)$ is calculated from Eq. (3.15) in three dimensions for $\chi = 1.00$, 1.75, 2.50, 3.25, and 4.00. $\Gamma_0/J = 2$. (b) The calculations of (a) are presented as log-log plots to illustrate the power-law frequency dependence of the ac conductivity in different frequency regimes. For $\chi < \chi^*$, $\sigma'(\omega)$ approaches a finite limit as $\omega \to 0$: the dc conductivity. For $\chi > \chi^*$, $\sigma'(\omega)$ vanishes as ω^2 for small ω. The transition occurs at $\chi^* \cong 2.373$. For $\omega/J \gg 1$, $\sigma'(\omega)$ decays as ω^{-2} for all χ. $\sigma_0 = 1$.

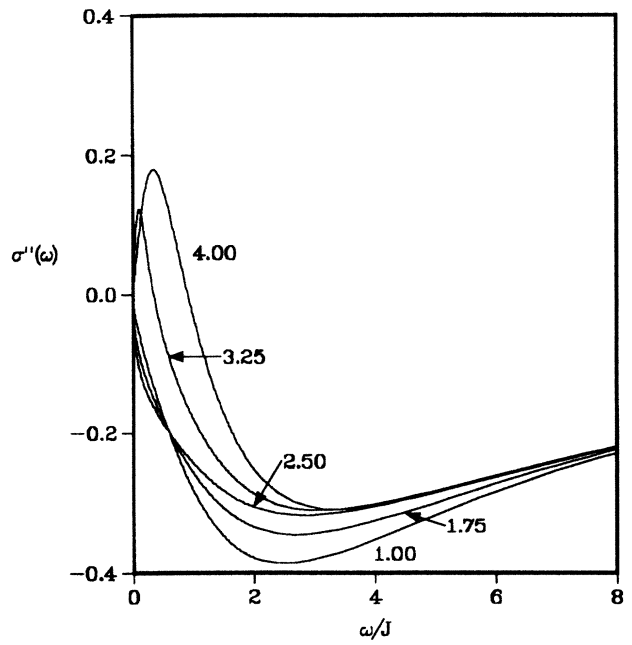

FIG. 4. The imaginary part of the complex conductivity $\sigma''(\omega)$ is calculated from Eq. (3.15) in three dimensions for the same values of χ that were used in Fig. 3. $\sigma_0=1$.

function of χ in Fig. 7. At $\chi=0$, which corresponds to the case of diffusive motion on an ordered lattice, $\sigma'(0)=\sigma_0$. Near χ^*, the dc conductivity vanishes as $1-\chi/\chi^*$, as can be seen from Eq. (3.12a).

We conclude by summarizing the implications of this work. The EDA is an analytical approach to treating the localization of a quantum particle moving in a random potential. It is based on the physical intuition that the ensemble-averaged density matrix of a particle moving in a random potential satisfies an effective Liouville equation which contains a generalized frequency-dependent dephasing rate $\Gamma(\epsilon)$. The EDA differs from many previous approaches to the quantum localization problem, in that the method focuses on the calculation of the ensemble-averaged density matrix, rather than the averaged wave function. It is conceptually similar to the recent treatments of transport in the Anderson problem.[15–17] $\Gamma(\epsilon)$ describes the loss of phase coherence between different points in space. By transforming to the Wigner representation [Eq. (2.9)], we see that $\Gamma(\epsilon)$ can be viewed as a generalized scattering rate in a Boltzmann equation with a BGK collision kernel. The effective Liouville equation is capable of describing coherent motion ($\Gamma=0$) and incoherent motion [when $\Gamma(0)$ is finite and large compared with the intersite coupling J]. The signature of localization is an infrared divergence in $\Gamma(\epsilon)$: $\Gamma(\epsilon)\sim\epsilon^{-\alpha}$. The success of the method in predicting a metal-nonmetal transition in the Anderson model validates our procedure. The correspondence between the EDA equation and the Boltzmann equation indicates that the applicability of the EDA method extends beyond the treatment of lattice

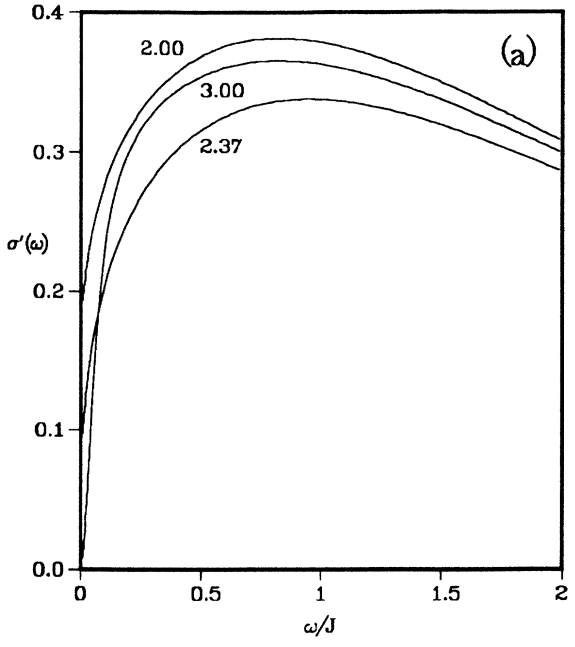

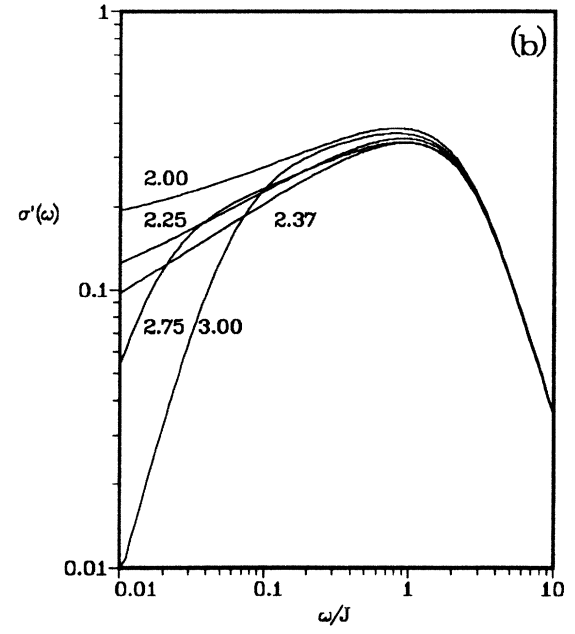

FIG. 5. (a) The ac conductivity $\sigma'(\omega)$ is calculated from Eq. (3.15) in three dimensions for $\chi=2.00$, 2.373, and 3.00. $\Gamma_0/J=2$. (b) The ac conductivity $\sigma'(\omega)$ is calculated from Eq. (3.15) in three dimensions for $\chi=2.00$, 2.25, 2.373, 2.75, and 3.00. The results are presented as log-log plots to illustrate the power-law frequency dependence of the ac conductivity in different frequency regimes. For $\chi<\chi^*$, $\sigma'(\omega)$ approaches a finite limit as $\omega\to 0$: the dc conductivity. For $\chi>\chi^*$, $\sigma'(\omega)$ vanishes as ω^2 for small ω. The transition occurs at $\chi^*\cong 2.373$. At $\chi=\chi^*$, $\sigma'(\omega)\sim\omega^{1/3}$ for $\omega/J\ll 1$. For $\omega/J\gg 1$, $\sigma'(\omega)$ decays as ω^{-2} for all χ. $\sigma_0=1$.

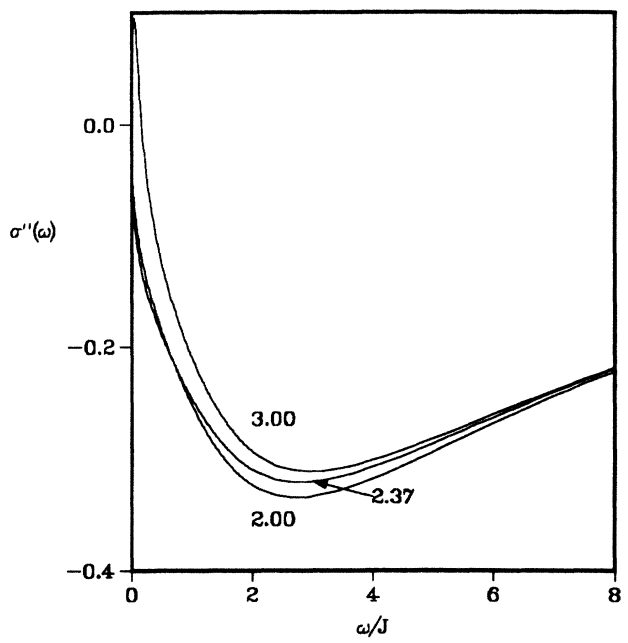

FIG. 6. The imaginary part of the complex conductivity $\sigma''(\omega)$ is calculated from Eq. (3.15) in three dimensions for the same values of χ that were used in Fig. 5(a). $\sigma_0=1$.

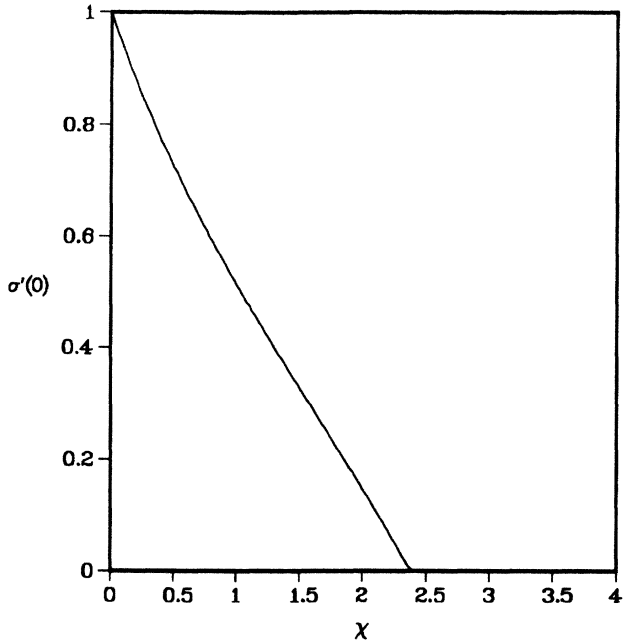

FIG. 7. The dc conductivity $\sigma'(0)$ is shown as a function of the disorder variable χ. For $\chi<\chi^*$, the motion of the electron is diffusive at long times, and $\sigma'(0)$ is finite. As χ approaches $\chi^*\cong 2.373$, $\sigma'(0)$ vanishes as $1-\chi/\chi^*$. For $\chi>\chi^*$, the electron is localized, and $\sigma'(0)$ is zero. $\sigma_0=1$.

models such as the Anderson problem to the general problem of the localization of a classical or quantum particle. This is one of the major advantages of the EDA. While the Anderson model is extremely valuable in providing an insight into the problem of transport in disordered systems, it is clearly oversimplified. Electronic motion in solids and glasses at finite temperatures is coupled to other degrees of freedom (e.g., phonons). Similarly, electronic motion in solutions involves coupling to internal molecular degrees of freedom. In addition, electron-electron interactions may affect the transport as well. The Anderson model, which treats a single particle in an external potential (static disorder), does not address the many-body aspects and the dynamical nature of the disorder in these systems. The present mapping of the ensemble-averaged equation of motion onto an effective Liouville (Boltzmann) equation is ideally suited for treating these more general types of disorder, and for developing a semiclassical theory of localization.

ACKNOWLEDGMENTS

The support of the U. S. National Science Foundation, the U. S. Office of Naval Research, the U. S. Army Research Office, and the donors of the Petroleum Research Fund is gratefully acknowledged. S. M. was partially supported by the Camille and Henry Dreyfus Fund.

*Present address: Department of Chemistry, Baker Laboratory, Cornell University, Ithaca, NY 14853.

[1]P. W. Anderson, Phys. Rev. **109**, 1492 (1958); R. Abou-Chacra, P. W. Anderson, and D. J. Thouless, J. Phys. C **6**, 1734 (1973).

[2]N. F. Mott and E. A. Davis, *Electronic Processes in Noncrystalline Materials* (Clarendon, Oxford, 1979).

[3]E. N. Economou and M. H. Cohen, Phys. Rev. B **5**, 2931 (1972).

[4]D. C. Licciardello and E. N. Economou, Phys. Rev. B **11**, 3697 (1975).

[5]D. J. Thouless, in *Ill-Condensed Matter*, edited by R. Balian, R. Maynard, and G. Toulouse (North-Holland, Amsterdam, 1979); *Anderson Localization*, edited by Y. Nagaoaka and H. Fukuyama (Springer, Berlin, 1982).

[6]E. Abrahams, P. W. Anderson, D. C. Licciardello, and T. V. Ramakrishnan, Phys. Rev. Lett. **42**, 673 (1979).

[7]P. Soven, Phys. Rev. **156**, 809 (1967); P. L. Leath, *ibid.* **171**, 725 (1968).

[8]F. Yonezawa and K. Morigaki, Suppl. Prog. Theor. Phys. **53**, 1 (1973).

[9](a) F. J. Wegner, Z. Phys. B **25**, 327 (1976); (b) D. Domany and S. Sarker, Phys. Rev. B **20**, 4726 (1979); S. Sarker and E. Domany, *ibid.* **23**, 6018 (1981).

[10]A. MacKinnon and B. Kramer, Phys. Rev. Lett. **47**, 1546 (1981).

[11]J. L. Pichard and G. Sarma, J. Phys. C **14**, L127 (1981); **14**, L617 (1981).

[12]A. Singh and W. L. MacMillan, J. Phys. C **17**, 2097 (1985).
[13]L. Root and J. L. Skinner, Phys. Rev. B **33**, 7738 (1986).
[14]B. Velicky, Phys. Rev. **184**, 614 (1969).
[15]W. Gotze, Philos. Mag. **43**, 219 (1981); D. Beilitz and W. Gotze, *ibid.* **43**, 517 (1981).
[16]D. Vollhardt and P. Wölfle, Phys. Rev. Lett. **45**, 842 (1980); **48**, 649 (1982); Phys. Rev. B **22**, 4666 (1980).
[17]H. Mueller and P. Thomas, Phys. Rev. Lett. **51**, 702 (1983). S. Mukamel, D. F. Franchi, and R. F. Loring, Chem. Phys. (to be published).
[18](a) R. F. Loring and S. Mukamel, Phys. Rev. B **33**, 7708 (1986); (b) R. F. Loring, M. Sparpaglione, and S. Mukamel, J. Chem. Phys. **86**, 2249 (1987); (c) S. Mukamel, D. F. Franchi, and R. F. Loring, Chem. Phys. (to be published).
[19]R. F. Loring and S. Mukamel, J. Chem. Phys. **85**, 1950 (1986).
[20]S. John, Phys. Rev. B **31**, 304 (1985).
[21]M. J. Stephen and G. Cwilich, Phys. Rev. B **34**, 7564 (1986).
[22]P. W. Anderson, Philos. Mag. B **52**, 505 (1985).
[23]H. Haken and G. Strobl, Z. Phys. **262**, 135 (1973).
[24]E. Wigner, Phys. Rev. **40**, 749 (1932); M. Hillery, R. F. O'Connell, M. O. Scully, and E. P. Wigner, Phys. Rep. **106**, 121 (1984).
[25]H. Mori, I. Oppenheim, and J. Ross, in *Studies in Statistical Mechanics*, edited by J. deBoer and G. E. Uhlenbeck (North-Holland, Amsterdam, 1962).
[26]P. L. Bhatnagar, E. P. Gross, and M. Krook, Phys. Rev. **94**, 511 (1954).
[27]H. Risken, *The Fokker-Planck Equation* (Springer, Berlin, 1984).
[28]G. Bergmann, Phys. Rep. **107**, 1 (1984).
[29]E. N. Economou, *Green's Functions in Quantum Physics* (Springer, Berlin, 1983).
[30]S. Katsura, T. Morita, S. Inawashiro, T. Horiguchi, and Y. Abe, J. Math. Phys. **12**, 892 (1971).
[31]G. S. Joyce, Philos. Trans. R. Soc. London, Ser. A **273**, 46 (1973).
[32]H. Stehfest, Commun. ACM **13**, 47 (1970); **13**, 624 (1970).